DNA 4503T

QUICK ESTIMATES OF PEAK OVERPRESSURE FROM TWO SIMULTANEOUS BLAST WAVES

R & D Associates
P. O. Box 9695
Marina del Rey, California 90291

December 1977

Topical Report for Period October 1977—December 1977

CONTRACT No. DNA 001-78-C-0009

THIS WORK SPONSORED BY THE DEFENSE NUCLEAR AGENCY
UNDER RDT&E RMSS CODE B310078464 P99QAXDB00136 H2590D.

Prepared for
Director
DEFENSE NUCLEAR AGENCY
Washington, D. C. 20305

Destroy this report when it is no longer needed. Do not return to sender.

PLEASE NOTIFY THE DEFENSE NUCLEAR AGENCY, ATTN: TISI, WASHINGTON, D.C. 20305, IF YOUR ADDRESS IS INCORRECT, IF YOU WISH TO BE DELETED FROM THE DISTRIBUTION LIST, OR IF THE ADDRESSEE IS NO LONGER EMPLOYED BY YOUR ORGANIZATION.

UNCLASSIFIED

SECURITY CLASSIFICATION OF THIS PAGE *(When Data Entered)*

REPORT DOCUMENTATION PAGE

READ INSTRUCTIONS BEFORE COMPLETING FORM

1. REPORT NUMBER: DNA 4503T
2. GOVT ACCESSION NO.
3. RECIPIENT'S CATALOG NUMBER
4. TITLE *(and Subtitle)*: QUICK ESTIMATES OF PEAK OVERPRESSURE FROM TWO SIMULTANEOUS BLAST WAVES.
5. TYPE OF REPORT & PERIOD COVERED: Topical Report for Period Oct [redacted]–Dec [redacted] 1977
6. PERFORMING ORG. REPORT NUMBER: RDA-TR-107006-008
7. AUTHOR(s): H. L. Brode
8. CONTRACT OR GRANT NUMBER(s): DNA 001-78-C-0009
9. PERFORMING ORGANIZATION NAME AND ADDRESS: R & D Associates, P.O. Box 9695, Marina del Rey, California 90291
10. PROGRAM ELEMENT, PROJECT, TASK AREA & WORK UNIT NUMBERS: Subtask P99QAXDB001-36
11. CONTROLLING OFFICE NAME AND ADDRESS: Director, Defense Nuclear Agency, Washington, D.C. 20305
12. REPORT DATE: Dec [redacted] 1977
13. NUMBER OF PAGES: 44
14. MONITORING AGENCY NAME & ADDRESS *(if different from Controlling Office)*: 44p.
15. SECURITY CLASS *(of this report)*: UNCLASSIFIED
15a. DECLASSIFICATION/DOWNGRADING SCHEDULE

16. DISTRIBUTION STATEMENT *(of this Report)*

Approved for public release; distribution unlimited.

DNA, SBIE; 4503T, AD-E300 340

17. DISTRIBUTION STATEMENT *(of the abstract entered in Block 20, if different from Report)*

18. SUPPLEMENTARY NOTES

This work sponsored by the Defense Nuclear Agency under RDT&E RMSS Code B310078464 P99QAXDB00136 H2590D.

19. KEY WORDS *(Continue on reverse side if necessary and identify by block number)*

Multibursts
Peak Overpressure
Reflected Pressure
Shock Interactions
Shock-on-Shock
Simultaneous Blast Waves
Target Coverage
Blast Waves

20. ABSTRACT *(Continue on reverse side if necessary and identify by block number)*

Several simple approximations to the peak overpressure between two interacting (simultaneous) blast waves are explored and compared to the LAMB approximation method for multibursts. The best estimates suggest about a 30% (10%-50%) increase in line-target coverage over that covered by two nonsimultaneous bursts. Coverage is restricted to strong shocks (ΔP > 100 psi).

Delta

DD FORM 1 JAN 73 1473 EDITION OF 1 NOV 65 IS OBSOLETE

UNCLASSIFIED

SECURITY CLASSIFICATION OF THIS PAGE *(When Data Entered)*

Table 1. Conversion Factors for U.S. Customary to Metric (SI) Units of Measurement

TO CONVERT FROM	TO	MULTIPLY BY
FOOT	METER	0.3048
MEGATON	TERAJOULE	4183
MILLISECOND	SECOND	0.001
PSI (POUNDSOFORCE/INCH^2)	KILO PASCAL (kPa)	6.894 757

TABLE OF CONTENTS

LIST OF FIGURES

LIST OF TABLES

SECTION 1. INTRODUCTION

Strong shocks in air reflect off rigid surfaces at many times (5-13 times) their original pressure. Opposing shocks of equal strength behave just as a reflected shock, leading to very high pressures at the initial point of contact. If two shocks of 100 psi collide, the resulting peak pressure is around 500. For two 1000-psi shocks, the peak pressure jumps to 8500 psi. This suggests that the area covered by a given overpressure from two simultaneous blast waves may be considerably larger than twice the area of a single burst.

Yet, while strong shock reflection factors are impressive, there is reason to believe that such high values do not extend far beyond the initial point of contact, and, further, two unequal shocks may interact in a much less impressive way. Strong blast waves are extremely transitory, and pressures, densities, and flow rates behind each blast front drop off exceedingly rapidly.

Careful considerations of such blast wave interactions lead directly to three-dimensional geometries which very much inhibit the accuracy and practical resolution achievable with canonical numerical methods. The following series of estimates, without benefit of rigorous modeling and detailed numerical calculations, are intended to bound the expectations for enhanced coverage by means of simultaneous blasts. Comparison is also made with the LAMB procedure,* as applied to two simultaneous bursts and the overpressures along the line joining their centers.

*Low-Altitude Multiple Burst.

SECTION 2. SEVERAL ESTIMATES

The peak overpressure from a single burst on the surface is well approximated with the formula [1]

$$\Delta P = \frac{3300\ W}{R^3} + \frac{192\ \sqrt{W}}{R^{3/2}} \text{ psi} \qquad (1)$$

with W the yield in megatons and R the distance in kilofeet.*

A normally reflected shock reaches a reflected pressure enhanced by the stagnation of the flow, and results in pressures for a strong shock much more than double the incident shock pressure. An approximate shock reflection factor for an ideal gas of specific heat ratio γ is given by

$$\frac{\Delta P_r}{\Delta P} = R = \frac{4\gamma P_o + (3\gamma - 1)\Delta P}{2\gamma P_o + (\gamma - 1)\Delta P} \qquad (2)$$

where ΔP is the incident overpressure, ΔP_r is the reflected overpressure, and P_o is the ambient pressure (14.7 psi). For sea level air, $1.1 < \gamma < 1.7$ ($\gamma \approx 1.3$ for $\Delta P \approx 1000$ psi) [1].

A more exact fit (within 3 percent) to this reflection factor is provided by the formula below, which accounts for the nonideal gas properties of sea level air [2].

*This formula agrees to within 10 percent with the accepted average of the nuclear test data which in turn are 90 percent contained by a spread of ±50 percent at pressures above 40 psi.

$$RF = \frac{0.002655\Delta P}{1 + 0.0001728\Delta P + 1.921 \times 10^{-9}\Delta P^2} + 2$$

$$+ \frac{0.004218 + 0.04834\Delta P + 6.856 \times 10^{-6}\Delta P^2}{1 + 0.007997\Delta P + 3.844 \times 10^{-6}\Delta P^2} \quad . \quad (3)$$

At the point where two simultaneous spherical blast waves meet, the peak overpressure can be fairly precisely described with these two approximations (Equations 1 and 3). For example (as in Figure 1), for two 1-MT simultaneous surface explosions separated by 6860 ft, the blast waves meet when each has a peak overpressure of 116 psi (Equation 1), and these shocks reflect at the point of contact to a pressure of 600 psi (a reflection factor of 5.18)(Equation 3). The value of 600 psi from a single 1-MT surface burst occurs at 1840 ft. For nonsimultaneous bursts, a separation of 3680 ft would cover a line target with more than 600 psi everywhere. The separation distance at which the interacting shocks reflect to 600 psi (6860 ft) is nearly twice as long.

The area associated with the region of enhanced blast pressures is a thin lens about the point of contact between spherical (or hemispherical) shocks, and is only a small fraction of the area covered by the individual blast waves.*

However, the use of the larger distance (6860 ft), where the shocks reflect to just 600 psi as an effective kill distance for a line target, is quite incorrect. The geometry of the situation (Figure 2) suggests that as the two shocks pass

*It is very wrong to assume that if the separation distance were increased by a factor of two, the area coverage would be correspondingly increased by a factor of four.

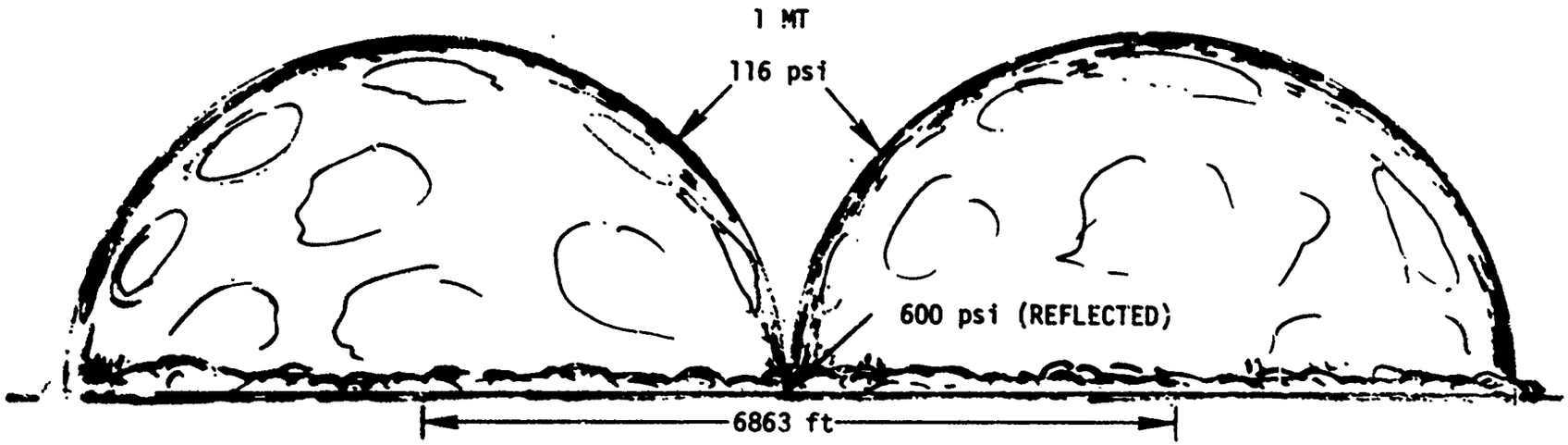

Figure 1. Two 1 MT Surface Bursts(Simultaneous) Reflecting to 600 psi

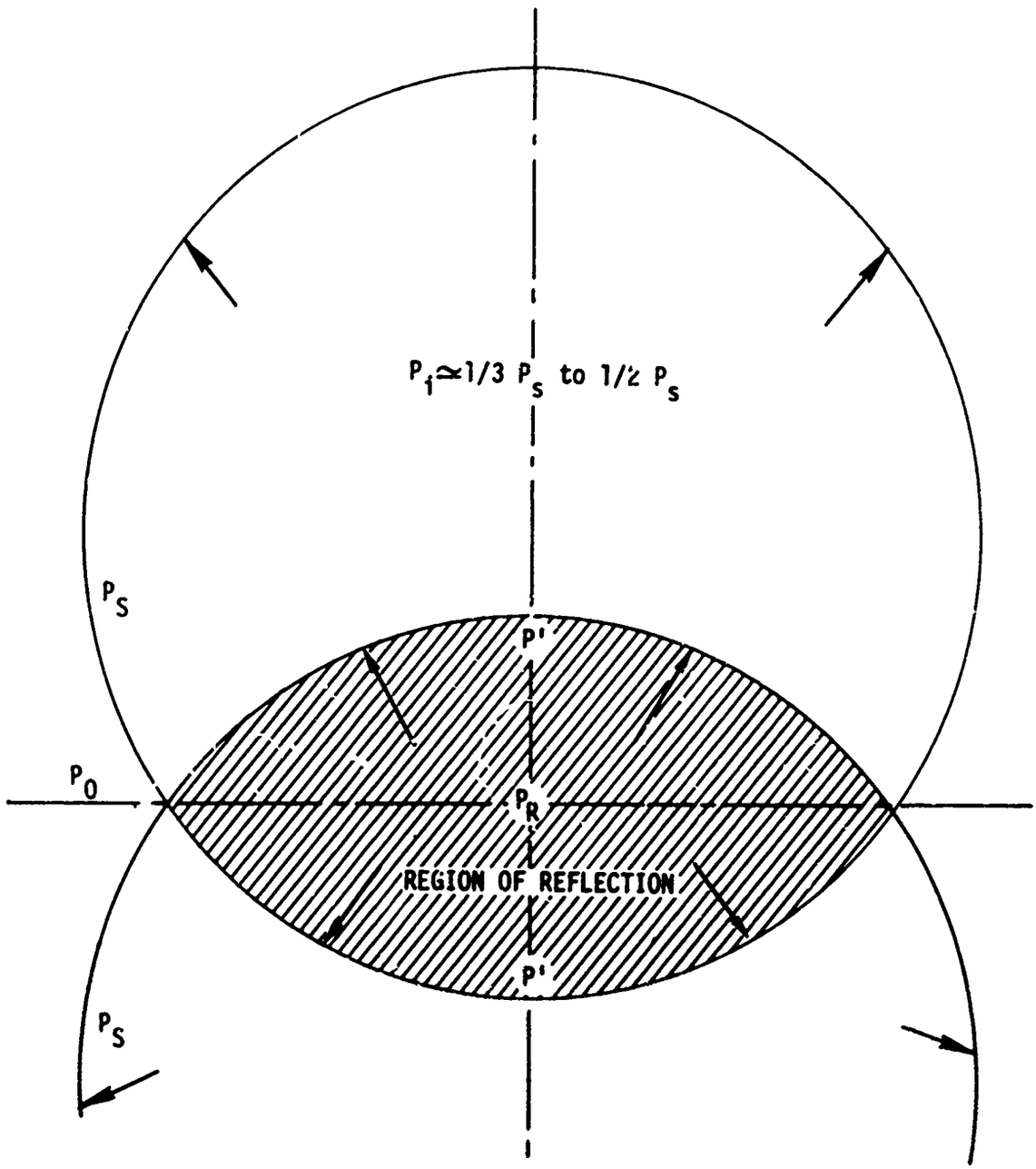

Figure 2. Geometry for Two Simultaneous Blast Waves Interacting

through each other, they continue to expand spherically, and so drop rapidly in pressure from that peak value of first contact (Figure 1). If their peak interaction gives only 600 psi, then all the region between burst points that lies beyond a radius from each burst point of 1840 ft would see less than 600 psi (Figure 3). That is, as in Figure 3, a total of 3200 ft would experience two shocks--both less than 600 psi.

Of greater interest is the separation distance that exposes the entire line target to more than 600 psi (or some other peak overpressure of interest). For this we need to know how rapidly these diverging shocks decrease in overpressure as they expand into each other. Since, on first contact with the opposing blast waves the transmitted shock starts at the peak reflection value, the initial value is well defined (Equation 3), but there does not exist an equally simple or direct formula for predicting the subsequent decay rate as the two blasts penetrate each other.

Numerical blast calculations provide detailed descriptions of the pressure field into which each transmitted shock is expanding and how it behaves in both space and time [3,4,5]. For most applications to hard targets (e.g., for 600-psi trenches), a simple strong shock model would suffice. In any case, while peak pressure decays with distance (as in Equation 1) approximately in proportion to the inverse cube of the distance, the interior of the fireball/blast-wave follows with a pressure about one-third to one-half of the shock value (Figure 4). In fact, both peak pressure and interior pressure decrease in proportion to the inverse of the time measured from the instant of explosion. An approximate relation is given by [2]*

*Two simpler but less exact forms for the pressure-time relation in a nuclear blast wave may be found in Reference 1, pp. 180-181.

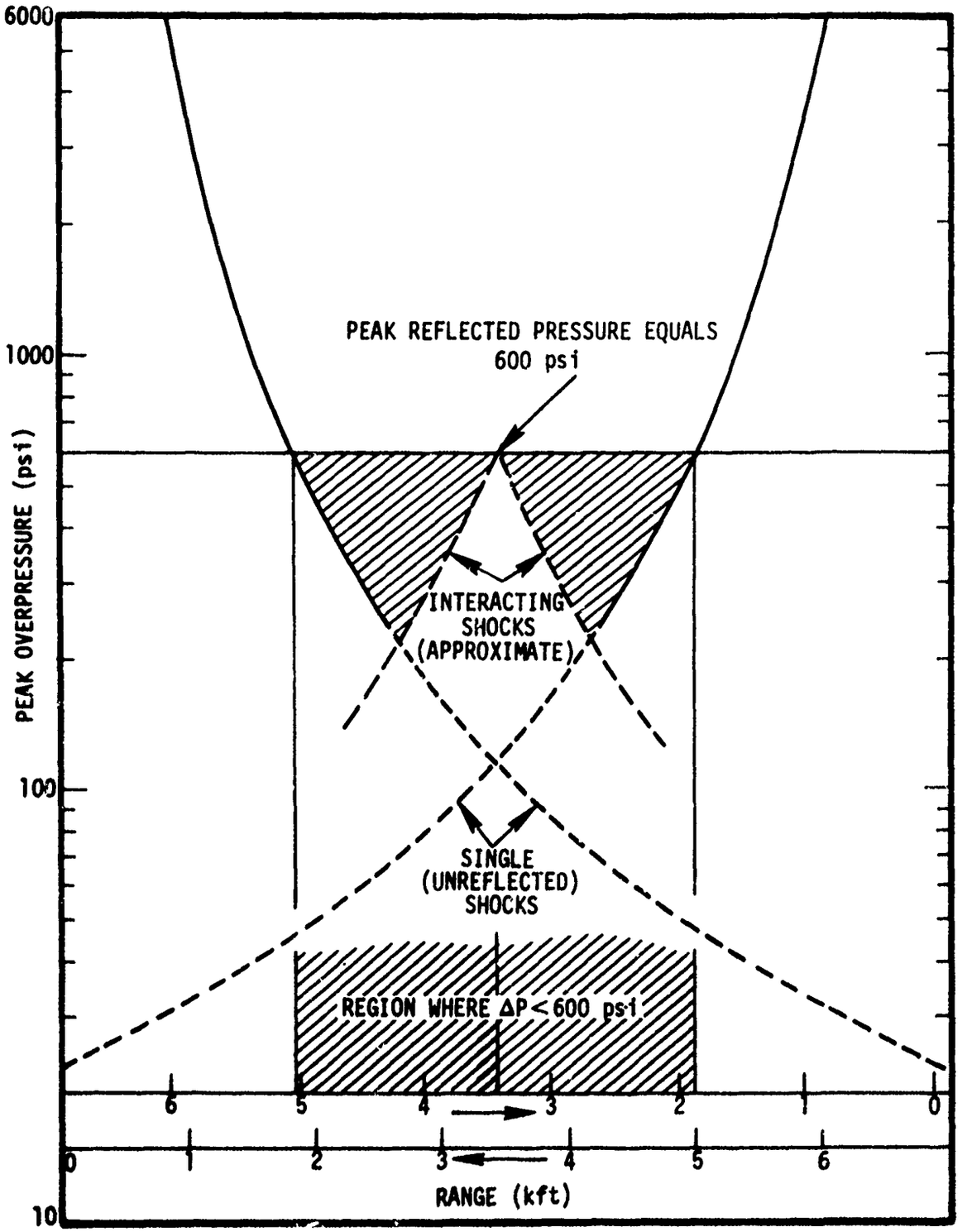

Figure 3. Peak Overpressure vs Range for Two 1 MT Simultaneous Surface Bursts Separated by 6860 ft

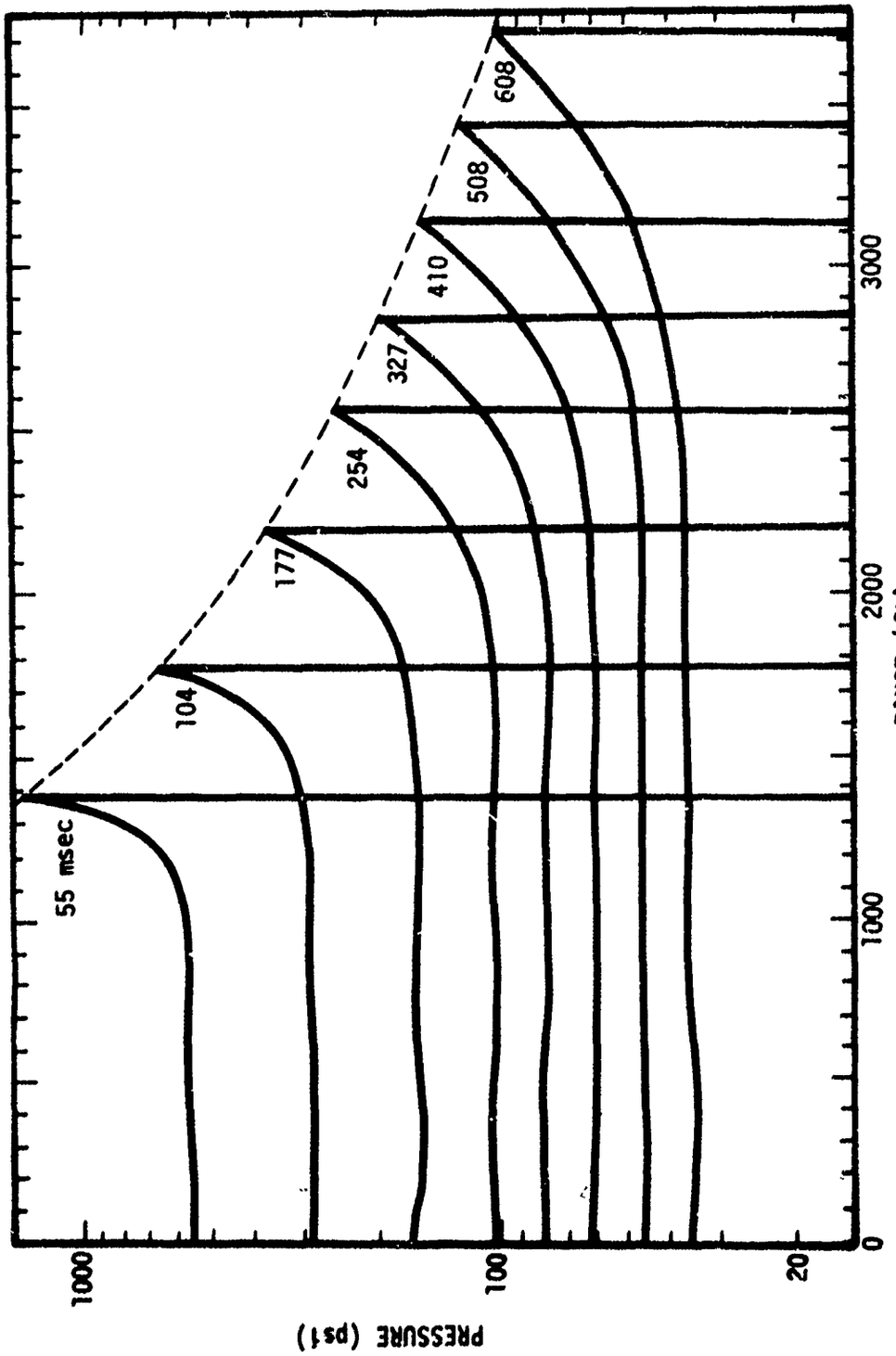

Figure 4. Pressure Profiles at Early Times for 1 MT Surface Bursts

$$\Delta P(t,T) \approx \left(\frac{148000}{0.135 + t}\right)\left[0.417 + 0.583\left(\frac{T}{t}\right)^6\right]\left(1 - \frac{t-T}{D}\right) f(t) \quad (4)$$

in which t is the time in msec (after burst), T is the shock arrival time (msec) for 1 MT, ($t \geq T$), D is the positive phase duration (msec) (the time during which the blast pressure is greater than ambient), and f(t) is an empirical adjustment fit of secondary importance.

$$f(t) = \frac{100 + 6.72t + 0.00581t^2}{100 + 18.8t + 0.0216t^2} \quad . \quad (5)$$

The essential time behavior of the pressure is illustrated by this approximation: The dominant behavior is a decay almost linear in time (more precisely as $\sim t^{-1.15}$) with a very sharp drop just behind the shock front to a value of about 40 percent of that at the front ($\sim t^{-6}$).

One possible approximation is to assume that the transmitted shock continues to generate the same peak reflection factor as it continues to expand and decrease inside the other blast wave. This is likely a gross overestimate of the off-peak pressures, since one might better use reflection factors appropriate to the transmitted shock as it continues to expand and decrease. The original blast that it is running into also continues to expand and decrease in pressure. A more correct approximation will account for this double decay, but, for the moment, consider several simple approximations for the transmitted peak overpressure.

Figure 5 shows several choices for these transmitted pressures in the particular case of two simultaneous surface

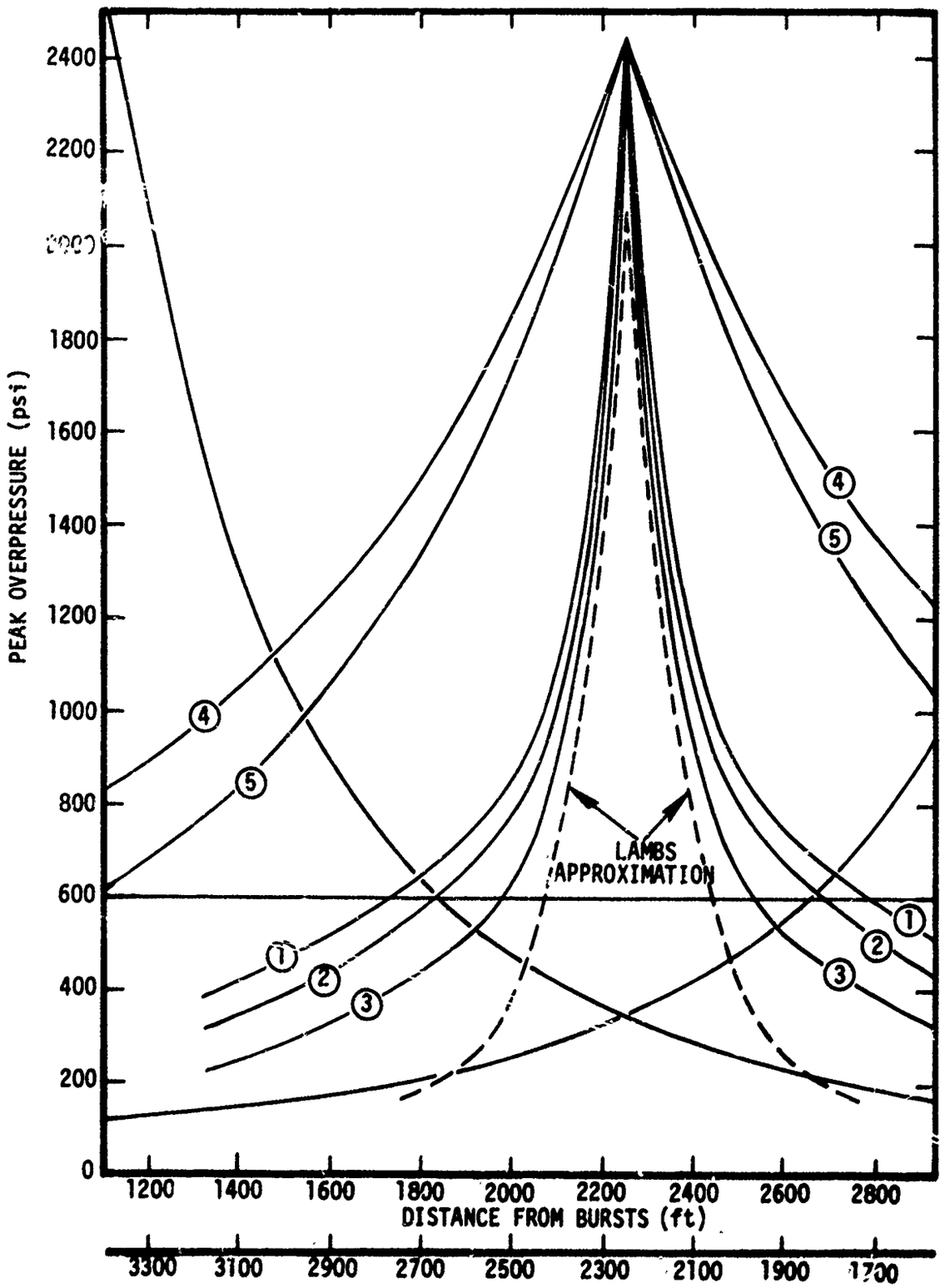

Figure 5. Approximations for the Peak Overpressure between Two Simultaneous 1 MT Surface Bursts 4500 ft Apart

bursts (1-MT) separated by 4500 ft. Table 2 illustrates the development of numerical values for each case.

(1) The peak interaction is defined as the local pressure in front of the transmitted blast wave multiplied by the initial reflection factor for the colliding shock fronts (reflection factor RF ≃ 7.0).

(2) The peak interaction pressure is defined as the local pressure in front of the transmitted blast wave multiplied by the reflection factor appropriate for a shock of strength equal to that of the second shock if it had expanded (unreflected) to that distance beyond the initial contact point.

(3) The peak interaction pressure is defined as the local pressure in front of the transmitted blast wave multiplied by the reflection factor for a shock of peak pressure equal to that pressure.

(4) The peak interaction pressure is defined as the unreflected (incident) shock pressure multiplied by the reflection factor appropriate to the time of first contact (RF ≃ 7.0).

(5) The peak interaction pressure is defined as the unreflected (incident) shock pressure multiplied by the reflection factor appropriate for that reduced shock strength as it expands in an undisturbed sea level atmosphere.

Table 2. 1-MT Simultaneous Burst Interaction (Separated by 4500 ft) Approximations to Peak Overpressure

① r_2 (ft)	② r_1 (ft)	③ ΔP_s (psi) $\Delta P(r_1)$	④ R_1 R(③) (Eqn 3)	⑤ R_2 R(⑥) (Eqn 3)	⑥ ΔP_i (psi) $\Delta P(r_2)$	CASE 1 ⑦ ΔP_R (psi) 7.0 x ⑥	CASE 2 ⑧ ΔP_R (psi) ④ x ⑥	CASE 3 ⑨ ΔP_R (psi) ⑤ x ⑥	CASE 4 ⑩ ΔP_R (psi) 7.0 x ③	CASE 5 ⑪ ΔP_R (psi) ③ x ④
2250	2250	350	7.0	7	350	2450	2450	2450	2450	2450
2120	2380	300	6.8	5.9	170	1190	1160	1000	2100	2040
1990	2510	260	6.6	5.2	120	840	790	620	1820	1720
1870	2630	230	6.4	4.9	100	700	640	490	1610	1470
1730	2770	200	6.2	4.6	80	560	500	370	1400	1240
1610	2890	180	6.0	4.4	70	490	420	300	1260	1080
1530	2970	168	5.8	4.2	65	455	380	270	1180	970
1420	3080	152	5.66	4.0	57	400	320	230	1060	610

None of these approximations account for the expansion of both shocks as they pass through each other. The most reasonable approximations are (3) and (2), but the others are shown for comparison (Figure 5).

The extra line target coverage for this example (1-MT bursts separated by 4500 ft) is listed in Table 3.

Table 3. Comparison of Range and Area Coverage Increases for Five Different Approximations to the Interaction of Two Simultaneous 1-MT Surface Bursts Separated by 4500 ft

APPROXIMATION NUMBER	PEAK OVERPRESSURE COVERED (psi)	SINGLE BURST RANGE (ft)	DISTANCE ADDED BY INTERACTION (ft)	RANGE INCREASE (%)
3[a]	540	1915	670	17
2[a]	610	1830	840	23
1	640	1800	910	25
5	990	1540	1410	46
4	1120	1470	1550	53

[a]MOST PLAUSIBLE APPROXIMATIONS.

The last two are clearly overestimates of the effect, but the first three may also predict more enhancement than is real.

Further estimates are given in the following sections.

SECTION 3. INTERACTION OF UNEQUAL SHOCKS

The preceding discussion has dealt with the case of two simultaneous bursts (equal strength shocks) interacting. Interactions between shocks of unequal strength are also of interest, since timing of multiple bursts may not be exact and the first blast may be considerably weaker by the time the second blast meets it.

Suppose two shocks meet when their respective peak overpressures are ΔP_1 and ΔP_2, and suppose the first is stronger than the second ($\Delta P_1 > \Delta P_2$). These shocks, on interacting, lead to an overpressure ΔP_R, a density ρ_R,* and a resultant particle velocity U_R. Figure 6 identifies the nomenclature in which two initial shocks have met and have resulted in two transmitted shocks which have velocities U_{R1} and U_{R2} directed away from each other, and a particle velocity U_R which is positive to the right if $\Delta P_1 > \Delta P_2$.

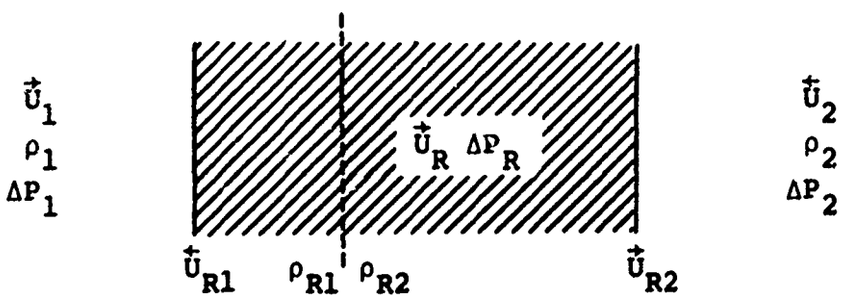

Figure 6. Shock Interaction Notation for Unequal Shocks

*Actually, two states of density and temperature separated by a contact discontinuity exist in the shock interaction region (shaded area, Figure 6), but pressure and velocity are the same in both states, viz., ΔP_R, U_R.

From standard shock relations, $\vec{U}_1$, $\vec{U}_2$, ρ_1, and ρ_2 are expressible in terms of ΔP_1 and ΔP_2 and are considered as known here.

$$U_1 = \Delta P_1 \left(\frac{(\gamma+1)}{2} \Delta P_1 + \gamma P_o \right)^{-1/2} \Big/ \sqrt{\rho_o}$$

$$U_2 = \Delta P_2 \left(\frac{(\gamma+1)}{2} \Delta P_2 + \gamma P_o \right)^{-1/2} \Big/ \sqrt{\rho_o}$$

$$\rho_1 = \rho_o \left[\left(\frac{(\gamma+1)}{2} \right) \Delta P_1 + \gamma P_o \right] \left[\left(\frac{(\gamma-1)}{2} \right) \Delta P_1 + \gamma P_o \right]^{-1}$$

$$\rho_2 = \rho_o \left[\left(\frac{(\gamma+1)}{2} \right) \Delta P_2 + \gamma P_o \right] \left[\left(\frac{(\gamma-1)}{2} \right) \Delta P_2 + \gamma P_o \right]^{-1} \quad . \qquad (6)$$

Expressing the conservation of mass flow rate through each shock, one may write

$$\rho_{R1}(U_{R1} + U_R) = \rho_1(U_1 + U_{R1}) \quad ,$$

$$\rho_{R2}(U_{R2} - U_R) = \rho_2(U_2 + U_{R2}) \quad . \qquad (7)$$

The momentum change related to the pressure jumps at the shocks can be expressed as

$$\Delta P_R - \Delta P_1 = \rho_1 U_1 (U_1 + U_{R1}) - \rho_{R1} U_R (U_R + U_{R1})$$

$$\Delta P_R - \Delta P_2 = \rho_2 U_2 (U_2 + U_{R2}) + \rho_{R2} U_R (U_{R2} - U_R) \quad . \qquad (8)$$

Eliminating U_{R1} and U_{R2} from Equations 6 and 7, one can write

$$\Delta P_R = \Delta P_1 + \frac{\rho_1 \rho_{R1}}{\rho_{R1} - \rho_1} (U_1 - U_R)^2$$

and

$$\Delta P_R = \Delta P_2 + \frac{\rho_2 \rho_{R2}}{\rho_{R2} - \rho_2} (U_2 + U_R)^2 \quad . \tag{9}$$

The initial energy density (E) jump conditions at each transmitted shock require

$$E_R - E_1 = \frac{P_R + P_1}{2} \left(\frac{1}{\rho_1} - \frac{1}{\rho_{R1}} \right)$$

and

$$E_R - E_2 = \frac{P_R + P_2}{2} \left(\frac{1}{\rho_2} - \frac{1}{\rho_{R2}} \right) \quad . \tag{10}$$

If one assumes an ideal gas with ratio of specific heats (γ), then $E = P/[(\gamma-1)\rho]$. Solving for ρ_R leads to

$$\frac{\rho_{R1}}{\rho_1} = \frac{(\gamma+1)\Delta P_R + (\gamma-1)\Delta P_1 + 2\gamma P_o}{(\gamma-1)\Delta P_R + (\gamma+1)\Delta P_1 + 2\gamma P_o}$$

and

$$\frac{\rho_{R2}}{\rho_2} = \frac{(\gamma+1)\Delta P_R + (\gamma-1)\Delta P_2 + 2\gamma P_o}{(\gamma-1)\Delta P_R + (\gamma+1)\Delta P_2 + 2\gamma P_o} \quad . \tag{11}$$

Using Equations 10 and the Hugoniot relations to express ρ_1, ρ_2, U_1, and U_2 in terms of ΔP_1 and ΔP_2 (Equation 6), one can derive

$$\Delta P_R = A \pm \sqrt{A^2 + C} \tag{12}$$

and

$$\Delta P_R = D \pm \sqrt{D^2 + F} \tag{13}$$

in which

$$A \equiv \Delta P_1 + \frac{\gamma+1}{4} \rho_1 (U_1 - U_R)^2$$

$$C \equiv -\Delta P_1^2 + \left(\frac{\gamma-1}{2} \Delta P_1 + \gamma P_o \right) \rho_1 (U_1 - U_R)^2$$

$$D \equiv \Delta P_2 + \frac{\gamma+1}{4} \rho_2 (U_2 + U_R)^2$$

$$F \equiv -\Delta P_2^2 + \left(\frac{\gamma-1}{2} \Delta P_2 + \gamma P_o \right) \rho_2 (U_2 + U_R)^2 \quad .$$

These equations can be solved for ΔP_R by iterative selection of the velocity U_R (all other values being predetermined by the values of γP_o, ΔP_1, and ΔP_2).

A set of example values of the resultant peak overpressure ΔP_R for two shocks meeting when one of them is 100 psi is illustrated in Figure 7 for two values of the specific heat ratio. For example, a 100-psi and a 500-psi shock meet to give more than 1500 psi for $\gamma = 1.4$ and about 2000 psi for $\gamma = 1.2$.

Figure 8 illustrates the peak pressure amplification from the meeting of two shocks with a plot of the ratio of the resulting peak overpressure to the sum of the two incident peak pressures. The amplification approaches unity if one of

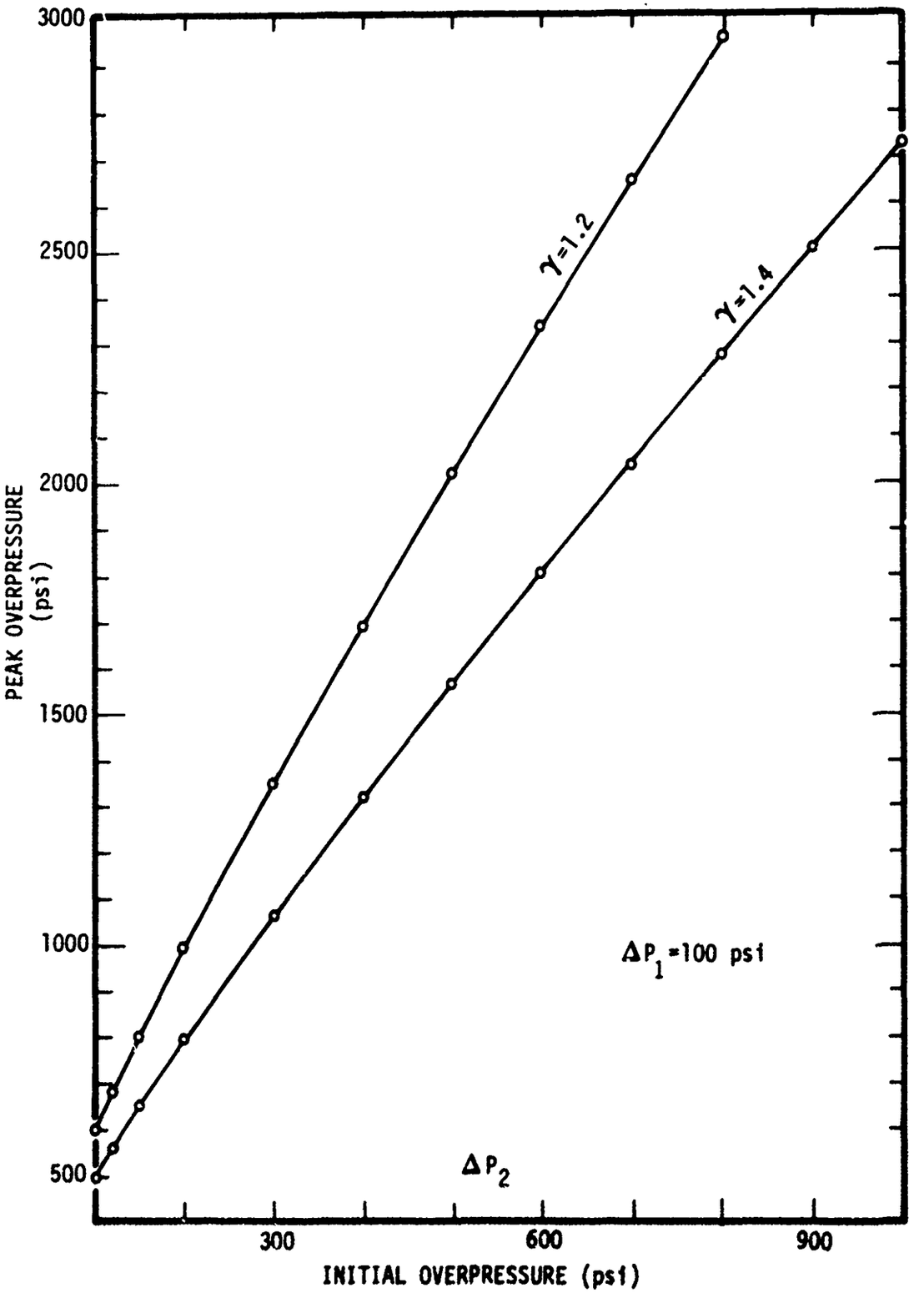

Figure 7. Resultant Peak Overpressure from Two Shocks (One at 100 psi)

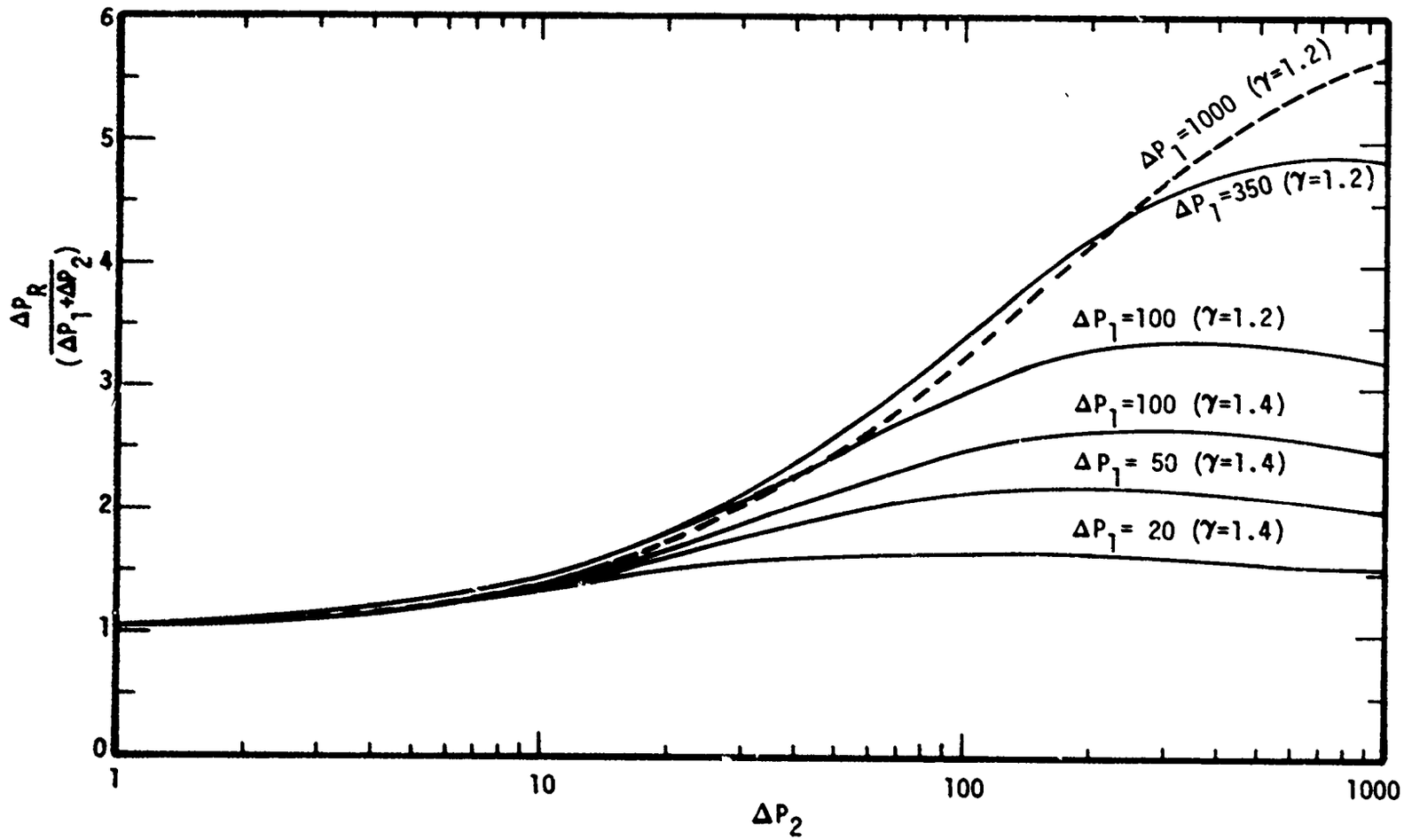

Figure 8. Shock Interaction between Unequal Shocks

the shocks is weak, and seems to reach a peak when the ratio of the two incident overpressures lies between 3 and 5.

This solution for the resultant peak pressure from the collision of two unequal shocks suggests yet another approximation to the peak overpressure distribution for our example of two simultaneous 1-MT bursts separated by 4500 ft (Figure 5). The interior overpressure (behind the shock front) that a transmitted shock encounters can be assumed to act similarly to a shock of that overpressure, and the resultant overpressure computed (by means of Equations 12 and 13). This approximation is tabulated in Table 4 and illustrated in Figure 9 (labeled Case 6).

This approximation, using unequal shock properties, is not very different from the simple average of the peak overpressures from the earlier bounding cases--Cases 3 and 5--which use the interior blast wave pressure multiplied by the normal shock reflection factor for that pressure (Case 3) and the single shock peak overpressure multiplied by its normal reflection factor (Case 5). This average is also shown in Figure 9 as Case 7.

Table 4. 1-MT Simultaneous Burst Interaction Peak Overpressure Approximations Using Unequal Shock Results

① r_2 (ft)	② r_1 (ft)	③ ΔP_s (psi) $\Delta P(r_1)$	⑥ ΔP_i (psi) $\Delta P(r_2)$	⑫ γ	CASE 6 ⑬ ΔP_R (psi) ΔP_R(③⑥)	⑭ ΔP_R ($\Delta P_s + \Delta P_i$) psi	CASE 7 ⑮ ΔP_R (psi) 9 + 11 (TABLE 1)
2250	2250	350	350	1.355	2460	7.0	2460
2120	2380	300	170	1.37	1450	3.1	1515
1990	2510	260	120	1.39	1070	2.8	1170
1870	2630	230	100	1.395	880	2.67	975
1730	2770	200	80	1.397	700	2.51	795
1610	2890	180	70	1.399	600	2.41	685
1530	2970	168	65	1.40	550	2.36	630
1420	3080	152	57	1.40	475	2.75	545

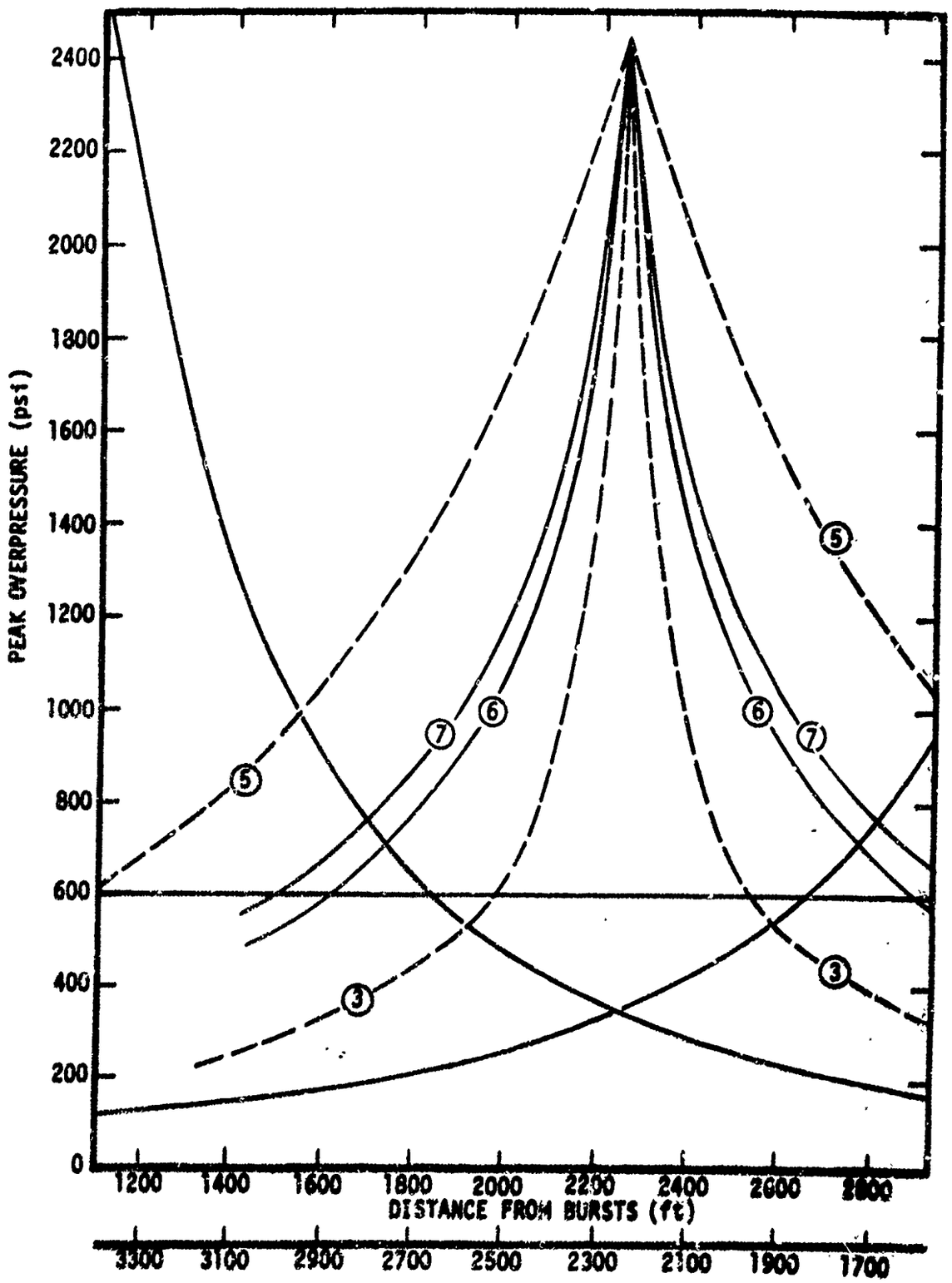

Figure 9. Further Approximations for the Peak Overpressure between Two Simultaneous 1 MT Surface Bursts 4500 ft Apart

SECTION 4. COMPARISON WITH THE LAMB PROCEDURE

A more careful accounting for the usual conservation of mass, momentum, and energy during these shock interactions requires some further assumptions and more geometry and arithmetic. Such an attempt is the basis of extensive calculations and predictions at the Air Force Weapons Laboratory with a program referred to as LAMB [6].

The essential features of this procedure are as follows: Mass conservation; assume:

$$\rho = \rho_o + \sum_{i=1}^{n} \Delta\rho_i, \quad (\rho \geq 0.5\ \rho_o) \tag{14}$$

in which ρ is the air density, ρ_o the ambient (pre-shock) air density, and $\Delta\rho_i$ is the over-density $(\rho_i - \rho_o)$ in each blast wave.

Recognize that densities in strong shock fronts may rise to more than ten times the ambient density, but may also fall to less than one-tenth the ambient value inside the fireball. This prescription predicts the peak density of two equal colliding strong shocks to be only about half of the correct Hugoniot value. (See Figure 10.)

The program, originally designed to approximate overlapping bursts at altitudes between 10 and 30 kft (in a missile defense role), quite arbitrarily restricts the underdensities (negative overdensities) to half (or more) of the ambient density. Such a restriction provides a reasonable, if unsatisfactorily empirical accounting of other dispersive

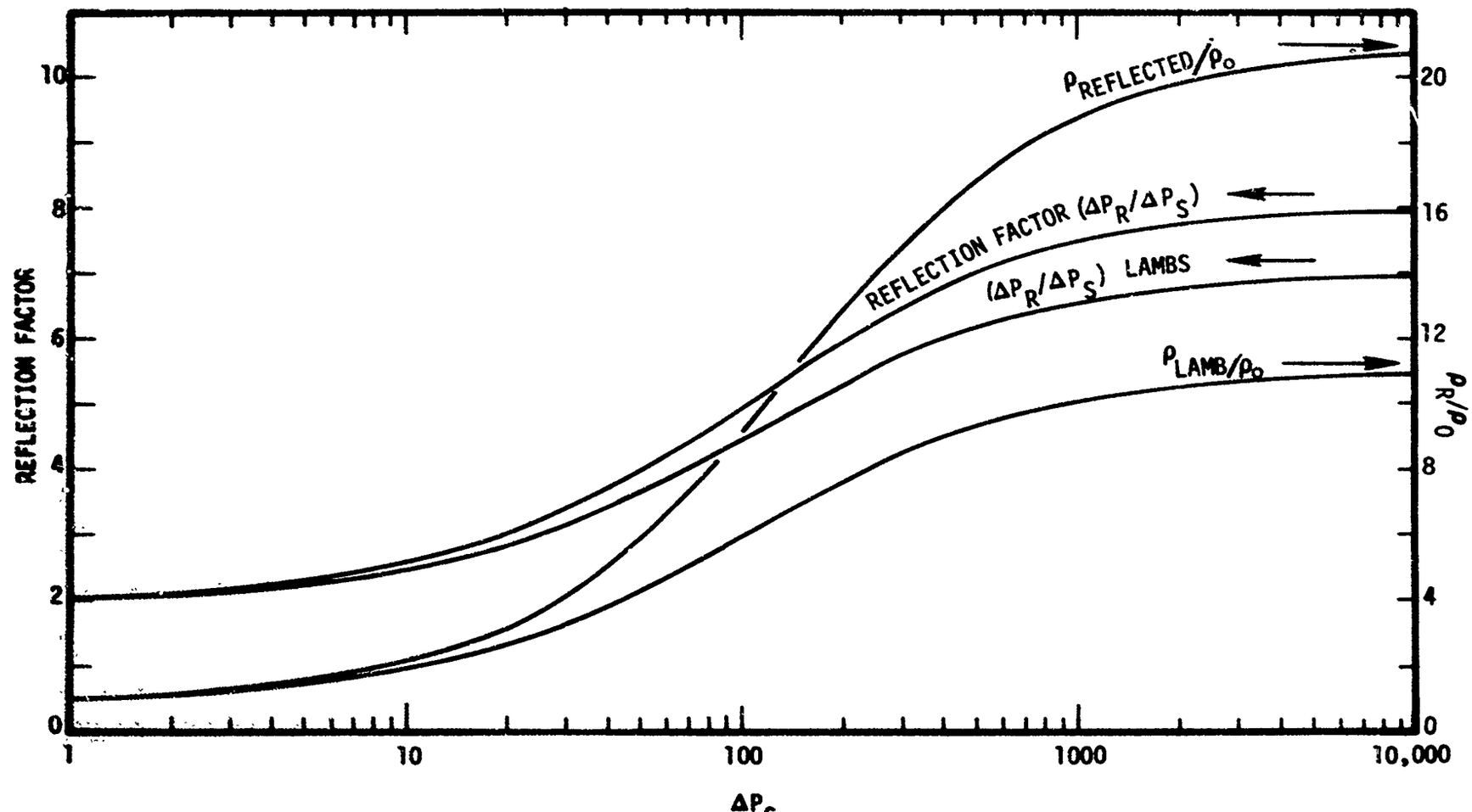

Figure 10. Comparison of Reflection Factor $(\Delta P_R/\Delta P_S)$ for Normal Shocks and by the Lambs Method; Comparison of Reflected Density and Density by Lambs Method

effects likely to occur in the high temperature (low density) interior of a nuclear fireball, but it cannot be justified rigorously (from first principles). Actually, some such limit is needed to prevent an undesired increase in net kinetic energy for a shock in the very low density interior of a strong blast wave (fireball) that would result otherwise from this prescription. Recognize also that this expression is not one of mass conservation, but prescribes density, or mass-per-unit volume. It has long been a favorite piece of magic for simplified blast solutions (many published as serious contributions) to make seemingly innocuous assumptions about density distributions and then proceed to unfold a marvelously consistent picture of some blast wave. The rabbit is always already in the hat here, however, since density distributions are, in fact, integral representations of the entire movement history of the blast, and the movements so described are a direct consequence of the acceleration or force (pressure gradient) history. So any density profile contains the blast wave history to that instant, and is not a trivially adjustable parameter of small consequence.

Conservation of momentum; assume:

$$\rho\vec{v} = \sum_{i=1}^{n} \rho_i \vec{v}_i \qquad (15)$$

where ρ_i is the density in the i^{th} blast wave, $\vec{v}_i$ is the particle velocity of the i^{th} blast wave, and ρ and $\vec{v}$ are the resultant density and particle velocity in the blast interactions. This represents a local momentum density vector sum without consideration of pressure impulse contributions, which is not quite consistent with the usual assumptions of inviscid gas dynamics for blast wave characterization.

Conservation of energy; assume:

$$\Delta P \equiv P - P_o = \sum_{i=1}^{n} \Delta P_i + \frac{1}{2}\left[\sum_{i=1}^{n} \rho_i v_i^2 - \rho v^2\right] \qquad (16)$$

in which $\Delta P_i \equiv P_i - P_o$ is the overpressure in the i^{th} blast, and ΔP is the resulting overpressure in the interacting blasts.

This prescription purports to convert excess kinetic energy from the opposing flows into pressure energy, a procedure consistent with normal hydrodynamic flow characterizations. However, it is inexact as an energy equivalent to add $1/2\ \rho v^2$ terms to overpressure. The dimensions are correct, but the compressibility factor $1/(\gamma-1)$ is missing. As a consequence, the reflection factor for two equal shocks resulting from this prescription is slightly in error. For an ideal gas:

$$\left(\frac{\Delta P_r}{\Delta P}\right)_{LAMB} = R_{LAMB} = \frac{2\gamma\Delta P + 4\gamma P_o}{(\gamma-1)\Delta P + 2\gamma P_o} \quad . \qquad (17)$$

More rigorously (as in Equation 3),

$$\frac{\Delta P_r}{\Delta P} = R = \frac{(3\gamma-1)\Delta P + 4\gamma P_o}{(\gamma-1)\Delta P + 2\gamma P_o} \quad . \qquad (18)$$

These two formulae are compared in Figure 10 for $1 < \Delta P < 10^4$, showing the LAMB procedure to be low by a factor of 7/8 at high overpressures ($\gamma = 1.4$).

The LAMB procedure, when applied to the previous example (two simultaneous 1-MT surface bursts 4500 ft apart), gives even less coverage with high pressure than the previous

estimates using peak reflection factors. As mentioned, the LAMB method misses the peak pressure by a factor approaching 7/8, and drops away from that peak value very rapidly (Figure 11). Table 5 compares the range enhancements from the approximations previously discussed with that for the LAMB model. The curves in Figure 11 and the basic data in Tables 2 and 4 are derived from Reference 1, but any of the descriptions in References 3, 4 or 5 would serve as well.

The added line coverage for this example with the LAMB procedure is about 11 percent, a smaller effect than any of the approximations given in the previous section. Good agreement with experiments is claimed for the LAMB model when applied to HE tests or to the shock reflections on a nuclear test such as PLUMBBOB-PRISCILLA. However, the arbitrary assumptions in the model are neither intuitive nor physically correct, and their effect on results far from the point of initial shock contact remains unclear.

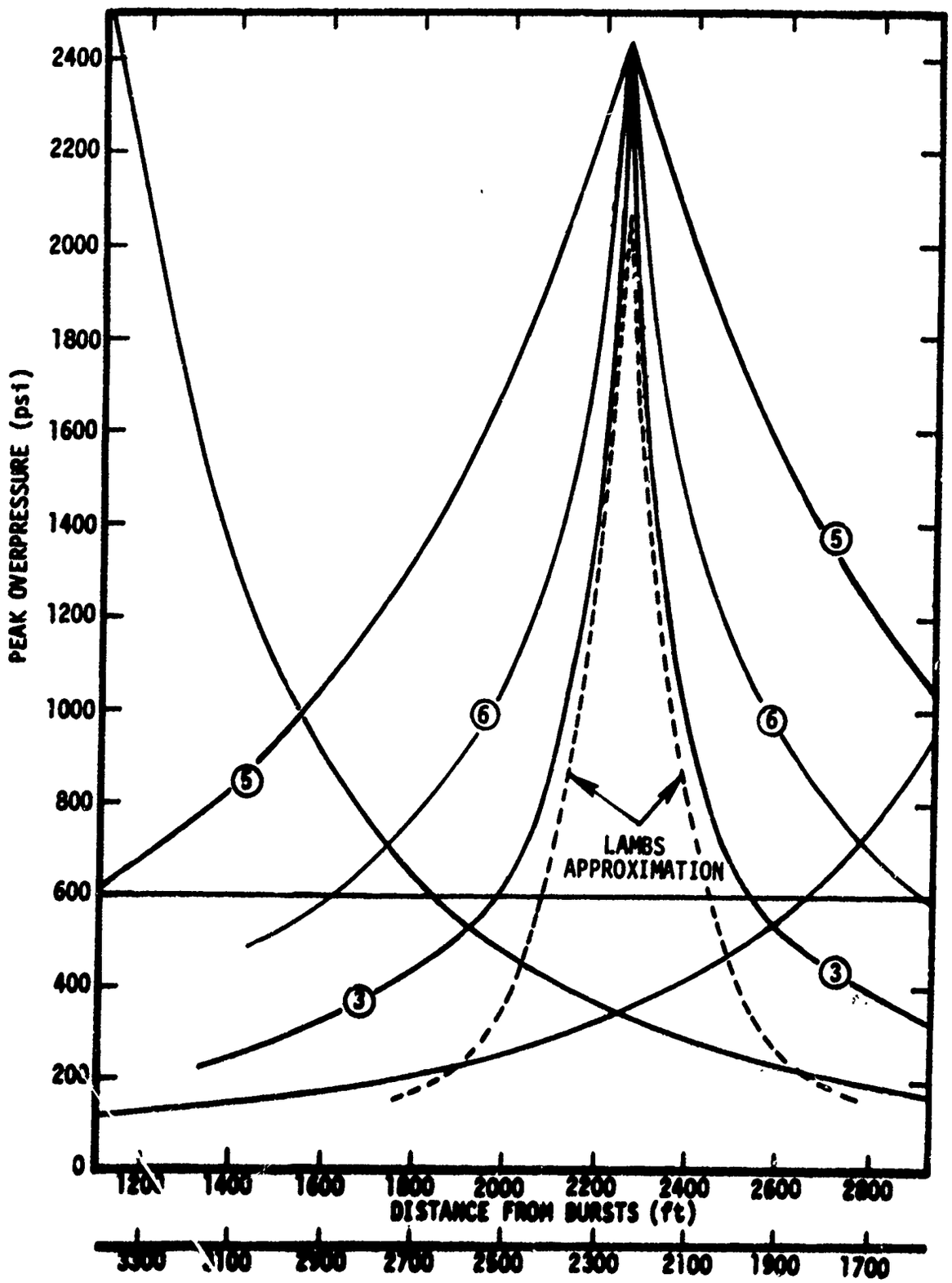

Figure 11. Approximations for the Peak Overpressure between Two Simultaneous 1 MT Surface Bursts 4500 ft Apart Compared with the LAMB Model

Table 5. Range Coverage Comparisons
(1-MT Bursts 4500 ft Apart)

APPROXIMATION CASE NUMBER	PEAK OVERPRESSURE COVERED (psi)	SINGLE BURST RANGE (ft)	DISTANCE ADDED BY INTERACTION (ft)	PERCENT RANGE INCREASE (%)
LAMB	450	2030	430	11
3	540	1915	670	17
6	710	1730	1040	30
5	990	1540	1410	35

SECTION 5. SUMMARY AND CONCLUSIONS

A reasonable lower limit approximation to the combined overpressure would appear to be to multiply the pressure at a point inside a single blast and in front of the transmitted shock from a second burst by the reflection factor for a shock of that interior pressure (Case 3). A similarly simple upper bound should be provided by multiplying the single blast peak overpressure by the normal reflection factor for that pressure at distances beyond the point of first contact for the two shocks (Case 5). A further procedure, almost as simple, providing an intermediate value, uses the pressure predicted for the interaction of unequal shocks, based on the pressure ahead of and behind the transmitted shock (Case 6).

The LAMB procedure is not rigorously correct, but it provides a more general and a more detailed treatment of interacting shocks. Unfortunately, it is not clear whether it overestimates or underestimates the resulting pressures, although all the predictions for this example lie above the LAMB-derived values. Accepting all the apparent uncertainty in these approximations to multiple shock interactions, one can still conclude that:

- The region of enhanced overpressures from two simultaneous separate blast waves is a small fraction of the area covered by each individual blast.

- The extra coverage of a line target with high overpressures (ΔP_s > 300 psi) is of the order of 10-50 percent, and, more probably, less than 30 percent.

- The LAMB procedure may, in some cases, underpredict the peak pressures for interacting blast waves.

REFERENCES

1. H. L. Brode, "Review of Nuclear Weapons Effects," Annual Review of Nuclear Science, Vol. 18, 1968, p. 180.

2. H. L. Brode, Height of Burst Effects at High Overpressures, DASA 2506, The Rand Corporation, RM-6301-DASA, 1970.

3. H. L. Brode, Point Source Explosion in Air, The Rand Corporation, RM-1824-AEC, 1956.

4. H. L. Brode, The Blast Wave in Air Resulting from a High Temperature, High Pressure Sphere in Air, The Rand Corporation, RM-1825-AEC, 1956.

5. C. E. Needham, M. L. Havens and C. S. Knauth, Nuclear Blast Standard (1 kT), Air Force Weapons Laboratory, Kirtland Air Force Base, New Mexico, AFWL-TR-73-55, (Revised) 1975.

6. C. E. Needham, Private Communication, Air Force Weapons Laboratory, Kirtland Air Force Base, New Mexico, November 1977.

DISTRIBUTION LIST

DEPARTMENT OF DEFENSE

Assistant to the Secretary of Defense
Atomic Energy
ATTN: Executive Assistant

Defense Advanced Rsch. Proj. Agency
ATTN: TIO
ATTN: NMRO
ATTN: PMO
ATTN: W. Whitaker
10 cy ATTN: STO

Defense Civil Preparedness Agency
Assistant Director for Research
ATTN: Staff Dir. Rsch., G. Sisson
10 cy ATTN: Admin. Officer

Defense Communications Agency
ATTN: Code 930
ATTN: CCTC/C672, F. Moore

Defense Documentation Center
Cameron Station
12 cy ATTN: TC

Defense Intelligence Agency
ATTN: DT-1C
ATTN: DB-4C, E. O'Farrell
ATTN: DT-2
ATTN: RDS-3A
ATTN: DI-7E

Defense Nuclear Agency
ATTN: DDST
2 cy ATTN: SPSS
4 cy ATTN: TITL

Department of Defense Explo. Safety Board
ATTN: T. Zaker

Field Command
Defense Nuclear Agency
ATTN: FCPR
ATTN: FCT
ATTN: FCTMOF

Joint Strat. Tgt. Planning Staff
ATTN: DOXT
ATTN: NRI-STINFO, Library
ATTN: XPFS
ATTN: JLTW-2

Livermore Division, Fld. Command, DNA
Lawrence Livermore Laboratory
ATTN: FCPRL

NATO School (SHAPE)
ATTN: U.S. Documents Officer

Under Secy. of Def. for Rsch. & Engrg.
ATTN: Strategic & Space Systems (OS)

WWMCCS System Engineering Org.
ATTN: T. Neighbors

DEPARTMENT OF THE ARMY

BMD Advanced Technology Center
Huntsville Office
ATTN: 1CRDABH-X
ATTN: CRDABH-S

BMD Program Office
ATTN: DACS-BMT, J. Shea

BMD Systems Command
ATTN: BMDSC-TEN, N. Hurst

Chief of Engineers
ATTN: DAEN-MCE-D
ATTN: DAEN-RDM

Deputy Chief of Staff for Ops. & Plans
ATTN: Dep. Dir. for Nuc. Chem. Matters
ATTN: MOCA-ADL

Deputy Chief of Staff for Rsch. Dev. & Acq.
ATTN: DAMA-AOA-M

Harry Diamond Laboratories
ATTN: DELHD-TI
ATTN: DELHD-NP

Redstone Scientific Information Ctr.
U.S. Army R&D Command
ATTN: Chief, Documents

U.S. Army Armament Material Readiness Command
ATTN: MA, Library

U.S. Army Ballistic Research Labs.
ATTN: DRDAR-BLE, W. Taylor
ATTN: DRXBR-X, J. Meszaros
ATTN: DRDAR-BLE, J. Keefer
2 cy ATTN: Technical Library

U.S. Army Communications Command
ATTN: Technical Reference Division

U.S. Army Engineer Center
ATTN: ATSEN-SY-L

U.S. Army Engineer Div., Huntsville
ATTN: HNDED-SR

U.S. Army Engineer Div., Ohio River
ATTN: ORDAS-L

U.S. Army Engr. Waterways Exper. Station
ATTN: J. Strange
ATTN: G. Jackson
ATTN: L. Ingram
ATTN: Library
ATTN: W. Flathau

U.S. Army Foreign Science & Tech. Ctr.
ATTN: Research & Concepts Branch

U.S. Army Missile R&D Command
ATTN: DRDMI-XS

DEPARTMENT OF THE ARMY (Continued)

U.S. Army Mat. & Mechanics Rsch. Ctr
ATTN: J. Mescall
ATTN: Technical Library
ATTN: R. Shea

U.S. Army Materiel Dev. & Readiness Cmd.
ATTN: DRCDE-D, L. Flynn
ATTN: DRXAM-TL

U.S. Army Mobility Equip. R&D Command
ATTN: DRDME-WC

U.S. Army Nuclear & Chemical Agency
ATTN: Library

U.S. Army War College
ATTN: Library

DEPARTMENT OF THE NAVY

Civil Engineering Laboratory
Naval Construction Battalion Center
ATTN: S. Takahashi
ATTN: R. Odello
ATTN: Code L08A

David W. Taylor Naval Ship R & D Ctr.
ATTN: Code L42-3

Naval Electronic Systems Command
ATTN: PME 117-21A

Naval Facilities Engineering Command
ATTN: Code 03A
ATTN: Code 04B
ATTN: Code 09M22C

Naval Ocean Systems Center
ATTN: E. Cooper
ATTN: Code 4471

Naval Postgraduate School
ATTN: Code 2124

Naval Research Laboratory
ATTN: Code 8440, F. Rosenthal
ATTN: Code 2627

Naval Sea Systems Command
ATTN: Code 03511
ATTN: ORD-913-13

Naval Ship Engineering Center
ATTN: NSEC 6105
ATTN: Code 09G3

Naval Surface Weapons Center
ATTN: Code F31

Naval Surface Weapons Center
Dahlgren Laboratory
ATTN: Technical Library & Information Services Branch

Naval War College
ATTN: Code E11

DEPARTMENT OF THE NAVY (Continued)

Naval Weapons Center
ATTN: P. Cordle
ATTN: C. Austin
ATTN: Code 533

Naval Weapons Evaluation Facility
ATTN: Code 10
ATTN: R. Hughes

Office of Naval Research
ATTN: Code 715
ATTN: Code 461, J. Warner
ATTN: Code 474, N. Perrone

Office of the Chief of Naval Operations
ATTN: OP 981
ATTN: OP 03EG

Director
Strategic Systems Project Office
ATTN: NSP-272
ATTN: NSP-43

DEPARTMENT OF THE AIR FORCE

Aerospace Defense Command/XPD
ATTN: XP
ATTN: XPDQQ

Air Force Geophysics Laboratory, AFSC
ATTN: LWW, K. Thompson

Air Force Institute of Technology
Air University
ATTN: Library

Air Force Systems Command
ATTN: DLCAW

Air Force Weapons Laboratory, AFSC
ATTN: DE-I
ATTN: DEX
ATTN: DES-S, M. Plamondon
ATTN: DES-C, R. Henny
ATTN: SUL
ATTN: J. Thomas
ATTN: C. Needham
ATTN: NT, J. Allen

Assistant Chief of Staff
Intelligence
ATTN: IN

Deputy Chief of Staff
Programs & Resources
ATTN: PRE

Deputy Chief of Staff, Rsch. & Dev.
ATTN: AFRDPI
ATTN: AFRDQSM

Commander
Foreign Technology Division
Air Force Systems Command
ATTN: NICD, Library

DEPARTMENT OF THE AIR FORCE (Continued)

Commander
Rome Air Development Center
Air Force Systems Command
ATTN: Documents Library/TSLD

Space & Missile Systems Organization/DE
Air Force Systems Command
ATTN: DEB

Space & Missile Systems Organization/DY
Air Force Systems Command
ATTN: DYS

Space & Missile Systems Organization/MN
Air Force Systems Command
ATTN: MNNH
ATTN: MMH

Strategic Air Command
ATTN: XPFS
ATTN: NRI-STINFO, Library

DEPARTMENT OF ENERGY

Albuquerque Operations Office
ATTN: Doc. Con. for Technical Library
ATTN: Doc. Con. for LBERI, C. Ortiz

Library Room G-042
ATTN: Doc. Con. for Classified Library

Nevada Operations Office
ATTN: Doc. Con. for Technical Library

Lawrence Livermore Laboratory
ATTN: Doc. Con. for Technical Information Dept. Library
ATTN: Doc. Con. for L-437, R. Schock
ATTN: Doc. Con. for L-90, R. Dong
ATTN. Doc. Con. for L-96, L. Woodruff
ATTN: Doc. Con. for L-7, J. Kahn
ATTN: Doc. Con. for L-90, D. Norris
ATTN: Doc. Con. for L-205, J. Hearst
ATTN: Doc. Con. for L-200, T. Butkovich

Los Alamos Scientific Laboratory
ATTN: Doc. Con. for A. Davis
ATTN: Doc. Con. for R. Bridwell
ATTN: Doc. Con. for Reports Library
ATTN: Doc. Con. for G. Spillman
ATTN: Doc. Con. for M. Sanford
ATTN: Doc. Con. for R. Whittaker

Oak Ridge National Laboratory
Union Carbide Corporation - Nuclear Division
X-10 Laboratory Records Department
ATTN: Doc. Con. for Technical Library
ATTN: Doc. Con. for Civil Defense Research Project

Office of Military Application
ATTN: Doc. Con. for Test Office

Sandia Laboratories
Livermore Laboratory
ATTN: Doc. Con. for Library & Security Classification Div.

DEPARTMENT OF ENERGY (Continued)

Sandia Laboratories
ATTN: Doc. Con. for 3141
ATTN: Doc. Con. for W. Roherty
ATTN: Doc. Con. for L. Hill
ATTN: Doc. Con. for A. Chaban
ATTN: Doc. Con. for L. Vortman

OTHER GOVERNMENT AGENCY

Department of the Interior
Bureau of Mines
ATTN: Technical Library

DEPARTMENT OF DEFENSE CONTRACTORS

Aerospace Corp.
ATTN: P. Mathur
ATTN: Technical Information Services
ATTN: H. Mirels

Agbabian Associates
ATTN: M. Agbabian

Analytic Services, Inc.
ATTN: G. Hesselbacher

Applied Theory, Inc.
2 cy ATTN: J. Trulio

Artec Associates, Inc.
ATTN: S. Gill

Avco Research & Systems Group
ATTN: Library

Battelle Memorial Institute
ATTN: Library
ATTN: R. Klingsmith

BDM Corp.
ATTN: Corporate Library
ATTN: A. Lavagnino

BDM Corp.
ATTN: R. Hensley

Boeing Co.
ATTN: Aerospace Library
ATTN: R. Carlson

Brown Engineering Company, Inc.
ATTN: M. Patel

California Research & Technology, Inc.
ATTN: S. Shuster
ATTN: K. Kreyenhagen
ATTN: Library

Calspan Corp.
ATTN: Library

Civil/Nuclear Systems Corp.
ATTN: J. Bratton

University of Dayton
Industrial Security Supvr, KL-505
ATTN: H. Swift

DEPARTMENT OF DEFENSE CONTRACTORS (Continued)

University of Denver
Colorado Seminary
Denver Research Institute
ATTN: Sec. Officer for J. Wisotski

EG&G Washington Analytical Services Center, Inc.
ATTN: Library

Gard, Inc.
ATTN: G. Neidhardt

General Electric Co.
Space Division
ATTN: M. Bortner

General Electric Co.-TEMPO
Center for Advanced Studies
ATTN: DASIAC

General Research Corp.
Santa Barbara Division
ATTN: B. Alexander

IIT Research Institute
ATTN: R. Welch
ATTN: M. Johnson
ATTN: Documents Library

Information Sciences, Inc.
ATTN: W. Dudziak

Institute for Defense Analyses
ATTN: Classified Library

J. H. Wiggins Co., Inc.
ATTN: J. Collins

Kaman AviDyne
Division of Kaman Sciences Corp.
ATTN: E. Criscione
ATTN: Library
ATTN: N. Hobbs

Kaman Sciences Corp.
ATTN: F. Shelton
ATTN: Library

Lockheed Missiles & Space Co., Inc.
ATTN: TIC, Library

Lovelace Biomedical & Environmental Research
Institute, Inc.
ATTN: R. Jones

Martin Marietta Corp.
Orlando Division
ATTN: G. Fotieo

McDonnell Douglas Corp.
ATTN: R. Halprin

Merritt CASES, Inc.
ATTN: J. Merritt
ATTN: Library

Meteorology Research, Inc.
ATTN: W. Green

DEPARTMENT OF DEFENSE CONTRACTORS (Continued)

Nathan M. Newmark
Consulting Services
ATTN: N. Newmark

Pacifica Technology
ATTN: R. Bjork
ATTN: G. Kent

Physics International Co.
ATTN: C. Vincent
ATTN: F. Sauer
ATTN: Technical Library
ATTN: D. Orphal
ATTN: E. Moore
ATTN: L. Behrmann

R & D Associates
ATTN: R. Port
ATTN: W. Wright, Jr.
ATTN: C. MacDonald
ATTN: J. Carpenter
ATTN: J. Lewis
ATTN: Technical Information Center
ATTN: C. Knowles
ATTN: A. Kuhl
10 cy ATTN: A. Latter
10 cy ATTN: H. Brode

R & D Associates
ATTN: H. Cooper

Rand Corp.
ATTN: C. Mow

Science Applications, Inc.
ATTN: Technical Library

Science Applications, Inc.
ATTN: J. Dishon

Science Applications, Inc.
ATTN: M. Knasel
ATTN: R. Sievers
ATTN: B. Chambers

Science Applications, Inc.
ATTN: D. Maxwell
ATTN: D. Bernstein

Southwest Research Institute
ATTN: W. Baker
ATTN: A. Wenzel

SRI International
ATTN: G. Abrahamson

Sundstrand Corp.
ATTN: C. White

Systems, Science & Software, Inc.
ATTN: Library
ATTN: D. Grine
ATTN: P. Riney
ATTN: T. Cherry
ATTN: K. Pyatt

DEPARTMENT OF DEFENSE CONTRACTORS (Continued)

Terra Tek, Inc.
ATTN: Library
ATTN: A. Jones
ATTN: S. Green

Tetra Tech., Inc.
ATTN: Library
ATTN: L. Hwang

TRW Defense & Space Sys. Group
ATTN: R. Plebuch
ATTN: P. Bhutta
ATTN: Technical Information Center
ATTN: D. Baer
ATTN: I. Alber
2 cy ATTN: P. Dai

TRW Defense & Space Sys. Group
San Bernardino Operations
ATTN: E. Wong

DEPARTMENT OF DEFENSE CONTRACTORS (Continued)

Universal Analytics, Inc.
ATTN: E. Field

Eric H. Wang
Civil Engineering Rsch. Fac.
ATTN: N. Baum
ATTN: L. Bickle

Weidlinger Assoc., Consulting Engineers
ATTN: M. Baron

Weidlinger Assoc., Consulting Engineers
ATTN: J. Isenberg

Westinghouse Electric Corp.
Marine Division
ATTN: W. Volz